Review of Scientific Instruments

A hybrid electrostatic retarding potential analyzer for the measurement of plasmas at extremely high energy resolution

Cite as: Rev. Sci. Instrum. **89**, 113306 (2018); https://doi.org/10.1063/1.5048926
Submitted: 18 July 2018 . Accepted: 25 October 2018 . Published Online: 20 November 2018

Glyn A. Collinson, Dennis J. Chornay, Alex Glocer, Nick Paschalidis, and Eftyhia Zesta

AIP Publishing

A hybrid electrostatic retarding potential analyzer for the measurement of plasmas at extremely high energy resolution

Glyn A. Collinson,[1,2,a)] Dennis J. Chornay,[1,3] Alex Glocer,[1] Nick Paschalidis,[1] and Eftyhia Zesta[1]

[1]*Heliophysics Science Division, NASA Goddard Space Flight Center, Greenbelt, Maryland 20771, USA*
[2]*Institute for Astrophysics and Computational Sciences, The Catholic University of America, Washington, District of Columbia 20064, USA*
[3]*University of Maryland College Park, 7403 Hopkins Avenue, College Park, Maryland 20742, USA*

(Received 18 July 2018; accepted 25 October 2018; published online 20 November 2018)

Many space plasmas (especially electrons generated in planetary ionospheres) exhibit fine-detailed structures that are challenging to fully resolve with the energy resolution of typical space plasma analyzers (10% → 20%). While analyzers with higher resolution have flown, generally this comes at the expense of sensitivity and temporal resolution. We present a new technique for measuring plasmas with extremely high energy resolution through the combination of a top-hat Electrostatic Analyzer (ESA) followed by an internally mounted Retarding Potential Analyzer (RPA). When high resolutions are not required, the RPA is grounded, and the instrument may operate as a typical general-purpose plasma analyzer using its ESA alone. We also describe how such an instrument may use its RPA to remotely vary the geometric factor (sensitivity) of a top hat analyzer, as was performed on the *New Horizons* Solar Wind at Pluto and *MAVEN* SupraThermal and Thermal Ion Composition instruments. Finally, we present results from laboratory testing of our prototype, showing that this technique may be used to construct an instrument with 1.6% energy resolution, constant over all energies and angles. *Published by AIP Publishing.* https://doi.org/10.1063/1.5048926

I. INTRODUCTION

One key parameter of any space plasma analyzer is its energy resolution. The finer the resolution is, the less the uncertainty is in the measurement of the energy of any given particle. However, often, the finer the resolution, the lower its sensitivity, the longer a sensor must integrate to obtain sufficient counting statistics, and thus the poorer the time resolution. Thus as with all aspects of the instrument design, energy resolution is a parameter which must be chosen carefully and traded off against other requirements. While there are instruments capable of varying their resolution in flight,[10] typically it is a fixed physical property that is set during design and cannot be altered after launch.

The decision of what energy resolution to bestow upon an instrument is often driven by where the instrument is going and what types of plasma distributions its designers expect it to encounter. For example, for instruments that measure the hot and rapidly changing magnetospheric plasmas (such as CLUSTER PEACE,[22] THEMIS[28] or the MMS FPI,[34] or Cassini CAPS[39]), fine energy resolution is far less important than the speed of measurement, and resolutions of 18%–20% are usually quite sufficient. When measuring a tight beam of particles (such as solar wind ions, field-aligned solar wind electron strahl, or a cold population of ionospheric ions coming in at the spacecraft ram velocity), plasmas cluster in a small range of energies, and a tighter energy resolution of around 10%–15% is required to accurately characterize the distribution.[31,35]

One type of plasma which greatly benefits from high resolution spectroscopy is the "photoelectrons" given off by planetary atmospheres. Bright mono-energetic ultraviolet emission lines in the solar spectrum ionize electrons in specific orbitals around neutral particles in the upper atmosphere, resulting in the emission of "photopeaks" at fixed discrete energies that are dictated by atomic physics.[16] Photoelectrons are important for the remote sensing of atmospheric photochemistry,[6] tracing magnetic field lines,[38] and tracing field-aligned potentials.[7,8,13] However, the individual spectral lines are so close together that they require very high energy resolution to resolve and separate. So far, the highest resolution measurements of photoelectrons[16,37] were obtained with the Photoelectron Spectrometer instrument aboard NASA's *Atmosphere Explorer E* spacecraft,[15] which achieved 2.5% energy resolution through heavy collimation of the incident electrons. While such high energy resolution reveals important features in exquisite detail, existing techniques to bestow 2.5% (or better) resolution upon an instrument will reduce the sensitivity of a plasma spectrometer so severely as to make it a highly specialized instrument. Thus, the majority of studies of photoelectrons have been performed by more general purpose instruments at lower resolution (8% → 13%).[1,23,30,31]

In this paper, we present a new technique for measuring space plasmas at up to 1.6% (full-width-half-maximum) energy resolution, in such a way that the full performance of the instrument may be restored when such high resolution is not required. While this technique was developed with the intent of measuring photoelectron peaks, it is broadly applicable for any situation where ultra-high resolution plasma spectrometery is required. Thus, while the prototype instrument described in

a)Electronic mail: glyn.a.collinson@nasa.gov

this paper was designed to measure electrons, it would work equally well for ions by reversing the polarity on the electrostatic charged-particle optics. Additionally, we describe how it bestows upon the instrument the additional ability to remotely vary the geometric factor (sensitivity) of the instrument, using a method flown as part of the Solar Wind at Pluto (SWAP) instrument aboard *New Horizons*.[27]

II. INSTRUMENT PRINCIPLE

Our new technique requires the combination of two common types of plasma instruments, an Electrostatic Analyzer (ESA) and a Retarding Potential Analyzer (RPA) [as shown in Fig. 2(a)]. We shall briefly review the operational principle behind each and then describe how we have combined them:

A. Electrostatic Analyzer (ESA)

The first component is a "top hat" electrostatic analyzer[4] (ESA), a standard instrument for the measurement of space plasmas. Top hat ESAs have flown on dozens (if not hundreds) of sounding rockets, satellites, and scientific spacecraft: at Earth;[5,22,28] the solar wind;[35] and to nearly every planet in the solar system.[1,2,19,26,27,33]

Plasma [green, Fig. 1(a)] enters the instrument through an aperture and passes through a set of two nested hemispherical metal plates. When a voltage is applied to the inner hemisphere

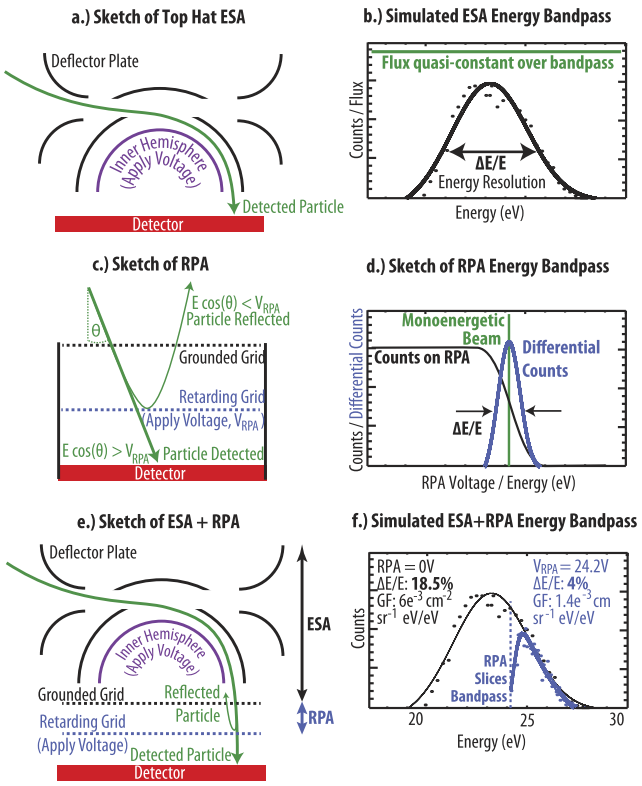

FIG. 1. Sketches showing the operational principles and energy response of ESA [(a) and (b)]; RPA [(c) and (d)]; and our new combination of an ESA + RPA [(e) and (f)]. (a) Sketch of top hat ESA. (b) Simulated ESA energy bandpass. (c) Sketch of RPA. (d) Sketch of RPA energy bandpass. (e) Sketch of ESA + RPA. (f) Simulated ESA+RPA energy bandpass.

(positive for electrons and negative for ions), the resulting electric field attracts the incoming particles toward the inner hemisphere. If the outward centripetal force of the particles approximately matches the attractive inward force from the electric field, the particles will "orbit" the hemispheres, strike the detector, and be counted. ESAs accept particles over a range of energies in a gaussian-like distribution [Fig. 1(b)]. We shall refer to this as the "*energy acceptance bandpass*." The energy resolution of an ESA is defined as the full-width at half-maximum (ΔE) of this bandpass, divided by the peak energy (E). The narrower the gap between the hemispheres, the narrower the range of energies that can traverse the instrument to be detected, and thus the finer the energy resolution. Altering the voltage on the inner hemisphere shifts the energy bandpass to a different peak energy (E). The total energy distribution of ambient plasma is built up by stepping the voltage on the inner hemisphere, measuring the number of counts at each step, and converting to flux.[11]

By itself, a top hat analyzer has a fixed field of view. Thus, many ESAs now incorporate electrostatic "deflector plates" on the exterior of the aperture.[1,3,5,12,25,34,36,40] Applying an electrostatic potential to the deflector plates steers the incoming beam of particles into the aperture, allowing the instrument to scan the sky without physically moving. The curved nature of the plates acts to pre-focus the particles entering the instrument, raising the focal point of the particles away from the detector. The greater the deflection, the further the motion of the focal point.[9]

B. Retarding Potential Analyzer (RPA)

A Retarding Potential Analyzer (RPA)[20,21,24,32] is a relatively simple device [Fig. 1(c)], employing two basic elements: a detector and a set of mesh grids which generate an electrostatic field which reflects incoming particles [Fig. 1(c)]. With no voltage applied to the grids, all ambient plasma is free to strike the detector. When a voltage is applied to the grid (V_{RPA}, negative for electrons and positive for ions), particles below a threshold energy (E_{RPA}) are repelled. Particles with energies equal to or greater than E_{RPA} have sufficient velocity to overcome it and strike the detector. The linear electric field generated by the RPA only applies force in one direction (tangential to the grids) and is most effective when particles are fired into the instrument parallel to the field. Thus, to the first order, the threshold energy of rejection ($|E|_{RPA}$) is given by Eq. (1), where q is the charge state of the particle,

$$|E|_{RPA} \approx \frac{q \cdot V_{RPA}}{\cos(\theta)}. \quad (1)$$

An RPA is an *integral* instrument, measuring the total flux of particles above its cut-off energy ($|E|_{RPA}$). By stepping the voltage on the grids (V_{RPA}), measuring the counts at each step, and then differentiating the result, it is possible to reconstruct the energy distribution of incident plasmas. For example, Fig. 1(d) shows how a monoenergetic and monodirectional beam (green line) of plasma appears to an RPA. When V_{RPA} is less than the energy of the beam, the beam may strike the detector, and the same number of counts is measured. As the voltage on the RPA approaches that of the beam, the counts

drop off to zero (black line) as the beam is repelled by the grids. For an RPA with infinitely fine resolution, this drop-off would be instantaneous. In reality, it occurs over a finite range of energies, corresponding to the energy resolution of the instrument. A simple way to determine this resolution using a monoenergetic beam is to record the counts vs. RPA voltage, differentiate [blue, Fig. 1(d)], and measure the full-width at half maximum [$\Delta E/E$, Fig. 1(d)].[17]

An RPA measures the total flux of all plasmas above its threshold energy ($\int_{E_{RPA}}^{\infty}$). Thus, while an RPA can have extremely high energy resolution, in practice it is challenging for an RPA alone to resolve fine plasma structures (such as photopeaks) unless they are the dominant component of the ambient plasma. If the total flux of a fine plasma distribution is small when compared to the total background flux, the "signal" of the change in counts as the RPA sweeps across them is very small when compared to the "noise" of the background. In this paper, we will show how an ESA can be used to put limits on the integration of an RPA and thus resolve fine features embedded within ambient space plasmas.

C. Combining an ESA with an RPA

Figure 1(e) shows a sketch of a hybrid plasma analyzer. Figure 1(f) shows simulations of the energy response of such an instrument. Particles first traverse the ESA, which provides an initial broad bandpass energy filter to incoming electrons (for the simulated instrument shown, $\Delta E/E$ = 18.5%). Particles then pass through a high-resolution retarding potential analyzer which may be electrically biased such that only electrons above a set threshold energy may reach the detector. If the threshold energy of the RPA ($|E|_{RPA}$) is set so that it coincides with the energy bandpass of the top hat analyzer, the RPA slices this bandpass with very high precision.

Such an instrument may take advantage of its inbuilt RPA in two ways:

1. As a direct variable geometric factor/energy resolution mechanism (as used on the *New Horizons* SWAP[27] and *MAVEN* STATIC instruments[29]) and
2. To scan the output of the ESA for fine features at the extremely high resolution of the RPA (the novel technique which is the focus of this paper).

Each shall now be discussed.

III. USING AN ESA/RPA AS A VARIABLE GEOMETRIC FACTOR/ENERGY RESOLUTION SYSTEM

One use of an RPA with an ESA is to vary the width and area of the energy bandpass, with remotely varying the geometric factor of the instrument.[10] Since the use of an RPA as a variable geometric factor system is already described in the literature,[27] it will now only be briefly described for completeness. Figure 1(f) shows the simulated energy response of a concept hybrid ESA/RPA instrument [Fig. 1(e)]. Note that these simulated results are purely illustrative and are shown *in lieu* of a rough sketch.

With the RPA off, the energy resolution of the instrument is that of the ESA (in this example, $\Delta E/E$ = 18.5% centered at 23 eV). When a voltage is applied to the RPA (in this example, 24 V), the energy bandpass of the instrument is narrowed (in this example, to $\Delta E/E$ = 4%). A byproduct of this is that the geometric factor (sensitivity) is reduced (in this case by 93%). An instrument operating in this mode would thus keep the voltages on the inner hemisphere and RPA in lock step, with both stepping simultaneously to keep the width of the energy bandpass ($\Delta E/E$) constant.

One disadvantage of using an RPA in this way as a variable geometric factor system is that it is only practical at low energies. This is because every additional electronvolt of energy range must be countered by an additional volt of potential difference on the RPA. Thus, an instrument with the typical ≈30 keV maximum energy for a top hat analyzer would also require a 30 kV sweeping high voltage supply to drive its outer RPA. With current technology, such a supply would be large, heavy, power hungry, and at risk of coronal discharge and high-voltage breakdown. Note that a more elegant approach to implement such a variable geometric factor system is to split the hemisphere into two sections and apply a differing polarization, as per the Mercury Electron Analyzers for the Bepi Colombo Mission.[36]

Notably, this technique was used by the Solar Wind Around Pluto (SWAP) instrument[27] which is flying aboard NASA's *New Horizons* mission. Note however that SWAP mounted the RPA at the entrance aperture (RPA/ESA), as opposed to between the ESA and the detector (ESA/RPA) as in this paper. The advantage of our configuration [Fig. 1(e)] is that particles exiting the ESA arrive at the RPA at a narrow range of incident angles [θ, Fig. 1(c)]. The narrower the range of incident angles, the sharper the cut-off in counts [see Eq. (1), Fig. 1(d)] and, thus, the finer the energy resolution of the combined instrument. Another advantage of this technique is that it minimizes the number of grids at the aperture. While important for restraining the electric fields from deflector plates,[14] extra grids introduce surfaces in the beam path on which unwanted particles (both charged particles and photons) can scatter into the field of view of the instrument and be detected.

Another top hat plasma analyzer which utilizes an externally mounted retarding potential analyzer is the SupraThermal and Thermal Ion Composition (STATIC) instrument[29] aboard NASA's *Mars Atmosphere and Volatile EvolutioN (MAVEN)* mission. STATIC uses an RPA to completely block off all but a thin slit of the aperture for each of its 32 azimuthal pixels, thus reducing the geometric factor without changing the shape of the energy bandpass.

IV. LABORATORY RESULTS: SCANNING AN RPA TO RESOLVE FINE-DETAILED STRUCTURE WITHIN THE ESA ENERGY BANDPASS

We shall now turn our attention back to the primary focus of this paper: describing and demonstrating experimentally how a combined ESA/RPA plasma analyzer may be operated to make extremely high energy resolution measurements. Whereas the *New Horizons* SWAP instrument used its externally mounted RPA as a variable geometric factor system, we use our internally mounted RPA to fine-scan the energy bandpass of the ESA, resolving the energy distribution within each

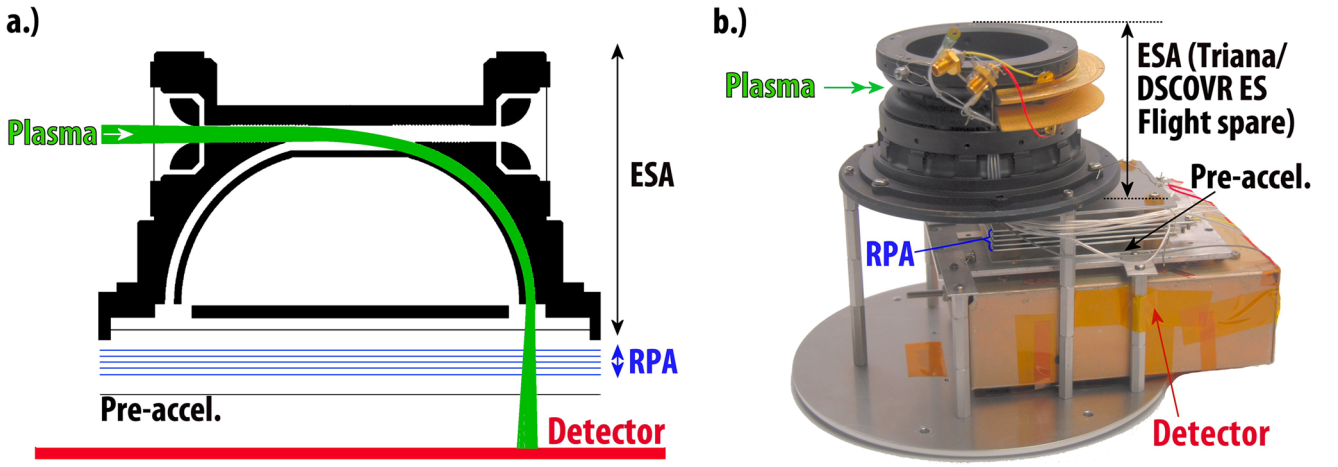

FIG. 2. (a) Simulation of prototype optics showing the Electrostatic Analyzer (ESA) first stage, Retarding Potential Analyzer (RPA) second stage, preacceleration grid, and detector. (b) Photograph of the experimental prototype, using a spare top-hat ESA from the *DSCOVR* (formerly *Triana*) electron spectrometer, and our very high resolution RPA designed after *Enloe and Shell*.[17]

ESA step and thus enabling extremely high energy resolution measurements of plasmas.

Figure 2(a) shows the cross section of simulation of our prototype instrument, expanding upon our initial conceptual sketch described previously [Fig. 1(e)], and Fig. 2(b) shows a photograph of the actual instrument itself. The instrument's electrostatic analyzer is a flight spare of the electron spectrometer flown aboard the NASA/NOAA *Deep Space Climate ObserVer* (DSCOVR, formerly *Triana*) mission. The instrument has a 10% energy resolution and a ±45° field of view using its pair of electrostatic deflector plates. The retarding potential analyzer, designed after *Enloe and Shell*,[17] consists of a series of five grids with a total transparency of ≈50%. Following *Enloe and Shell*,[17] the use of five grids, with V_{RPA} applied to the middle three and $0.9V_{RPA}$ applied to the outer two, produces an extremely high resolution RPA (1.6% in our case, demonstrated shortly). Following the RPA is a single grid to which a static voltage (+200 V for electrons and −200 V for ions) is applied to pre-accelerate the particles into the detector. For a particle detector, we chose to use an off-the-shelf Quantar beam imager for convenience in the testing of this laboratory prototype.

Figure 3 shows results from the laboratory testing of our prototype hybrid ESA/RPA instrument. Monoenergetic beams of electrons were fired into the aperture [green arrow, Fig. 2(b)]. The instrument was physically rotated over its entire range of angular acceptance, and at each elevation, the voltage on the inner hemisphere was stepped to cover the entire energy acceptance bandpass of the ESA. At each combination of elevation and energy, the voltage on the RPA was stepped in 0.1 V increments until no counts were measured on the detector. This experiment was repeated for three different energies of beam (50 eV, 100 eV, 200 eV) and at three deflection angles (undeflected, +24°, +45°) using the DSCOVR-ES deflector plates.

Figure 3(a) shows a plot of the unprocessed data. Each point represents a flight-like measurement where particles are incident into the instrument over the entire energy and angular acceptance bandpass of the instrument. The x-axis shows the voltage on the RPA (as a percentage of the energy of the

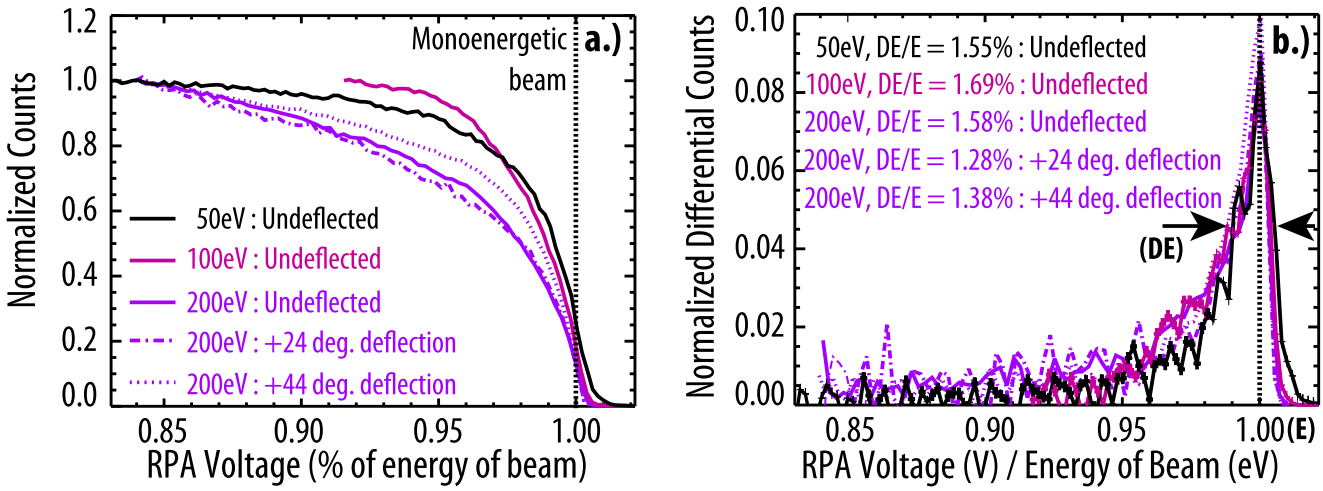

FIG. 3. (a) Laboratory data from our prototype, showing the change in RPA counts (normalized to RPA off) with RPA voltage as a percentage of the energy of the beam. (b) Differential RPA counts, showing that we may now resolve the beam with the 1.6% energy resolution of the RPA.

beam), and the y-axis shows counts on the detector. Since the beam flux was not constant from one experiment to the next, counts have been normalized against their starting condition since it is the *rate of change* in counts that is important when measuring plasma distributions with an RPA. Thus, while on the first appearance each plot might appear to have a different gradient, as will shortly be shown, this is simply the result of this normalization.

Figure 3(b) shows a plot of the differential of counts vs. V_{RPA} normalized to the beam energy in order to determine the energy resolution of the instrument. As in our earlier concept sketch [Fig. 1(d)], the combined ESA/RPA prototype instrument resolves the beam with a peak at precisely the correct energy. Moreover, the energy resolution of the instrument was extremely stable (≈1.6%) over all energies and deflection angles. Charged particle simulations of our prototype have shown that while the deflector plates of the ESA shift the focal point of the instrument (as with all top hat analyzers with deflector plates[9]), they do not greatly affect the angular distribution of particles as they strike the RPA. Thus, since the energy and angular distribution of electrons entering the RPA has not changed, the energy resolution remains constant.

V. SIMULATED RESULTS: MEASURING PHOTOELECTRONS WITH A COMBINED ESA AND RPA

Finally, we describe an example of how such an instrument might be used to measure the energy spectra of a space plasma at very high resolution. Figure 4(a) shows the simulated spectra of photoelectrons at Earth, as calculated by the Polar Wind Outflow Model,[18] exhibiting the bright discrete photopeaks described previously. Dashed black lines correspond to the four most prominent photopeaks.

Figure 4(b) shows the energy acceptance bandpass of the instrument. Each blue curve represents the acceptance bandpass of the ESA alone, and each red curve shows the total bandpass of the instrument when a retarding voltage is applied to the RPA. For each step of the ESA, the RPA is first set so that it coincides with the center energy of the ESA bandpass (E_0). The voltage on the RPA is then stepped in 0.1 V increments until it reaches the energy corresponding to the full-width at half maximum of the ESA bandpass ($E_0 + \Delta E/2$). Then the voltage on the ESA is incremented, bringing its central energy to match the energy of the RPA. Then the process repeats. Dashed blue lines show the central energy of each ESA step.

Figure 4(c) shows the raw counts that would be measured by the instrument at each RPA step. When this is differentiated [Fig. 4(d)], the original energy spectra are recovered, and the energies of each photopeak may be directly measured.

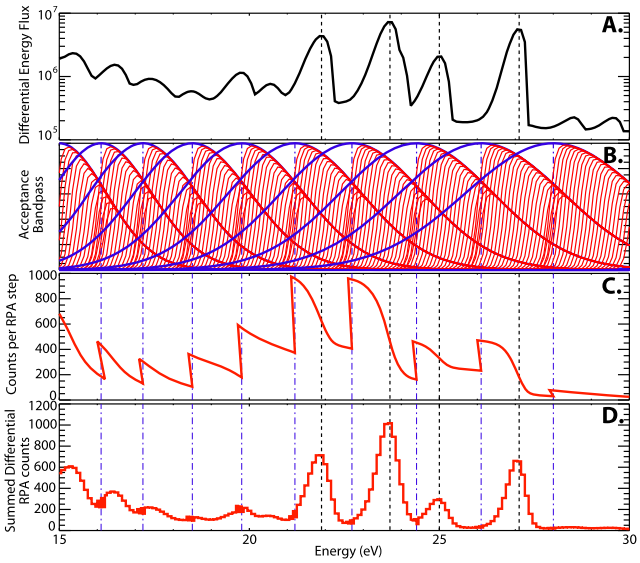

FIG. 4. (a) Simulation of the Earth's photoelectron spectra at 800 km; (b) acceptance bandpass of the instrument; (c) counts per ESA/RPA step; (d) de-convolved spectra of photoelectrons.

VI. DISCUSSION AND CONCLUSIONS

In this brief report, we presented a concept for how a Retarding Potential Analyzer (RPA) may be placed between the output of a top hat Electrostatic Analyzer (ESA) and a particle detector to create an instrument with extremely high energy resolution. Energy scanning is performed in two stages. Particles entering the instrument first pass through the ESA, which provides an initial broadband energy filter of 10% → 20% (depending on the optics) and puts limits on the integration of the RPA. Particles then pass through the RPA, which scans over the energy bandpass of the ESA and resolves the fine structure within. We presented the results of laboratory testing of our prototype hybrid ESA/RPA instrument, showing that we were able to resolve a monoenergetic beam to within 1.6%. While we have specifically applied this new technique to the measurement of electrons, it would be equally effective with ions, and all that would be needed to measure would be to reverse the polarity of the voltages on the ESA and RPA.

Such a technique would bestow two capabilities upon a flight instrument. First, the ability to remotely vary the geometric factor of the instrument (up to the limits of the power supply for the RPA), as on the *New Horizons* Solar Wind At Pluto (SWAP) instrument.[27] Second, through scanning its RPA, the ability to resolve fine features within the ambient plasma distribution to extremely high resolution.

The disadvantages of this system are threefold. First, the space taken up by the RPA requires moving the detector below the optimal focus point of the existing optics. Thus, the ESA must be either specially optimized to lower the focal point or suffer from degraded azimuthal resolution. Second, even when the RPA is off, the ≈50% transparency of its grids will reduce the sensitivity of the instrument. Third, scanning with the RPA requires repeating each measurement at every RPA step, and thus we must exchange higher energy resolution for longer scans (than if we were operating the ESA alone) and poorer time resolution. However, this last concern is mitigated by the fact that we may control this after launch and remotely command the instrument to freely make this trade-off in flight.

We observe that the energy distribution function [Fig. 3(b)] of our prototype exhibits a pronounced low energy tail. There are two possible contributing factors to this tail.

First, *Enloe and Shell*,[17] from whose work our five-grid RPA was designed, also reported such a feature and found that it was the result of the non-uniformity of the grids. They reported that such a tail could be minimized (and the response function was made to be close to optimal) by optimizing the ratio in voltage between the two outer grids of the RPA and the three inner grids [in our experiment 0.9 V (outer grids) to 1 V (inner grids)]. Second, this tail may be a result of the angular distribution of particles exiting the ESA, in which case the problem could potentially be mitigated by optimizing the geometry of the top-hat electrostatic analyzer.

Finally, we will now briefly compare this new technique for increasing the energy resolution of a top hat analyzer with an alternative scheme employed on an existing instrument, the *MAVEN* Solar Wind Electron Analyzer (SWEA).[31] Electrons entering SWEA first pass through two concentric toroidal grids, onto which a potential difference of 0 to −25 V may be set. This decelerates incoming particles, reducing their energy. Since the energy resolution of a top hat is fixed ($\Delta E/E$), this effectively increases the energy resolution. For example, with no potential drop applied to the grids, a 27 eV electron measured by SWEA's 17% energy resolution is resolved to within ±2.3 eV (27 * 0.17 = 4.59 = ±2.3). If a −25 V retarding potential is applied to SWEA's aperture grids, the electron is decelerated to 2 eV and now may be measured to within ±0.17 eV. While this approach does not suffer from the shortcomings of our new combined ESA/RPA (as described above), pre-decelerating particles in this way come with their own disadvantages. First, any particles with energies less than the grid potential are repulsed and not measured. Second, any increase in the energy resolution (f) using this technique comes at the cost of a reduction in the square of the geometric factor (f^2). Thus, if modest improvements in energy resolution (cf. SWEA uses its grid to improve $\Delta E/E$ from 17% to 12%) are needed, then a SWEA-like external repulsive grid is a very sound technique. However, if extremely high energy resolutions (e.g., <5%) are required, then on balance the ESA/RPA technique outlined in this paper would be a better approach.

ACKNOWLEDGMENTS

We thank Sara Riall, Nyugen Long, and Timothy Cameron for their engineering expertise. We thank David Mitchell for useful discussions. This research was partly supported by Internal Research and Development funding at NASA Goddard Space Flight Center.

[1]S. Barabash *et al.*, "The analyzer of space plasmas and energetic atoms (ASPERA-3) for the Mars express mission," Space Sci. Rev. **126**, 113–164 (2006).
[2]S. Barabash *et al.*, "The analyser of space plasmas and energetic atoms (ASPERA-4) for the Venus express mission," Planet. Space Sci. **55**, 1772–1792 (2007).
[3]J. L. Burch, R. Goldstein, T. E. Cravens, W. C. Gibson, R. N. Lundin, C. J. Pollock, J. D. Winningham, and D. T. Young, "RPC-IES: The ion and electron sensor of the Rosetta Plasma Consortium," Space Sci. Rev. **128**, 697–712 (2007).
[4]C. W. Carlson, D. W. Curtis, G. Paschmann, and W. Michel, "An instrument for rapidly measuring plasma distribution functions with high resolution," Adv. Space Res. **2**, 67–70 (1982).
[5]C. W. Carlson, J. P. McFadden, P. Turin, D. W. Curtis, and A. Magoncelli, "The electron and ion plasma experiment for FAST," Space Sci. Rev. **98**, 33–66 (2001).
[6]A. J. Coates, S. M. E. Tsang, A. Wellbrock, R. A. Frahm, J. D. Winningham, S. Barabash, R. Lundin, D. T. Young, and F. J. Crary, "Ionospheric photoelectrons: Comparing Venus, Earth, Mars and Titan," Planet. Space Sci. **59**, 1019–1027 (2011).
[7]A. J. Coates, A. Wellbrock, J. H. Waite, and G. H. Jones, "A new upper limit to the field-aligned potential near Titan," Geophys. Res. Lett. **42**, 4676–4684, https://doi.org/10.1002/2015GL064474 (2015).
[8]G. Collinson *et al.*, "Electric Mars: The first direct measurement of an upper limit for the Martian 'polar wind' electric potential," Geophys. Res. Lett. **42**, 9128–9134, https://doi.org/10.1002/2015GL065084 (2015).
[9]Collinson, G. A., "The computer simulated design of an improved plasma analyser towards an electron spectrometer for solar orbiter," Ph.D. thesis, Mullard Space Science Laboratory, Department of Physics and Astronomy, University College London, 2010.
[10]G. A. Collinson and D. O. Kataria, "On variable geometric factor systems for top-hat electrostatic space plasma analyzers," Meas. Sci. Technol. **21**(10), 105903 (2010).
[11]G. A. Collinson *et al.*, "The geometric factor of electrostatic plasma analyzers: A case study from the fast plasma investigation for the magnetospheric multiscale mission," Rev. Sci. Instrum. **83**(3), 033303 (2012).
[12]G. A. Collinson *et al.*, "Hot flow anomalies at Venus," J. Geophys. Res.: Space Phys. **117**(A16), A04204, https://doi.org/10.1029/2011ja017277 (2012).
[13]G. A. Collinson *et al.*, "The electric wind of Venus: A global and persistent 'polar wind'-like ambipolar electric field sufficient for the direct escape of heavy ionospheric ions," Geophys. Res. Lett. **43**, 5926, https://doi.org/10.1002/2016GL068327 (2016).
[14]G. A. Collinson, J. P. McFadden, D. J. Chornay, D. Gershman, and T. E. Moore, "Constraining electric fields from electrostatic deflector plates: A brief report and case study from the fast plasma investigation for the magnetospheric multiscale mission," J. Geophys. Res.: Space Phys. **121**, 7887–7894, https://doi.org/10.1002/2016JA022590 (2016).
[15]J. P. Doering, C. O. Bostrom, and J. C. Armstrong, "The photoelectron-spectrometer experiment on atmosphere explorer," Radio Sci. **8**, 387–392, https://doi.org/10.1029/RS008i004p00387 (1973).
[16]J. P. Doering, W. K. Peterson, C. O. Bostrom, and T. A. Potemra, "High resolution daytime photoelectron energy spectra from AE-E," Geophys. Res. Lett. **3**, 129–131, https://doi.org/10.1029/GL003i003p00129 (1976).
[17]C. L. Enloe and J. R. Shell II, "Optimizing the energy resolution of planar retarding potential analyzers," Rev. Sci. Instrum. **63**, 1788–1791 (1992).
[18]A. Glocer, N. Kitamura, G. Toth, and T. Gombosi, "Modeling solar zenith angle effects on the polar wind," J. Geophys. Res.: Space Phys. **117**, A04318, https://doi.org/10.1029/2011JA017136 (2012).
[19]J. S. Halekas, E. R. Taylor, G. Dalton, G. Johnson, D. W. Curtis, J. P. McFadden, D. L. Mitchell, R. P. Lin, and B. M. Jakosky, "The solar wind ion analyzer for MAVEN," Space Sci. Rev. **195**, 125–151 (2015).
[20]W. B. Hanson, D. R. Zuccaro, C. R. Lippincott, and S. Sanatani, "The retarding-potential analyzer on atmosphere explorer," Radio Sci. **8**, 333–339, https://doi.org/10.1029/RS008i004p00333 (1973).
[21]W. B. Hanson, R. A. Heelis, R. A. Power, C. R. Lippincott, D. R. Zuccaro, B. J. Holt, L. H. Harmon, and S. Sanatani, "The retarding potential analyzer for dynamics explorer-B," Space Sci. Instrum. **5**, 503–510 (1981).
[22]A. D. Johnstone *et al.*, *PEACE: A Plasma Electron and Current Experiment* (ESA Special Publication, 1993), Vol. 1159, p. 163.
[23]N. Kitamura, K. Seki, Y. Nishimura, N. Terada, T. Ono, T. Hori, and R. J. Strangeway, "Photoelectron flows in the polar wind during geomagnetically quiet periods," J. Geophys. Res.: Space Phys. **117**, A07214, https://doi.org/10.1029/2011JA017459 (2012).
[24]W. C. Knudsen, K. Spenner, J. Bakke, and V. Novak, "Pioneer Venus orbiter planar retarding potential analyzer plasma experiment," IEEE Trans. Geosci. Remote Sens. **18**, 54–59 (1980).
[25]R. P. Lin *et al.*, "A three-dimensional plasma and energetic particle investigation for the wind spacecraft," Space Sci. Rev. **71**, 125–153 (1995).
[26]D. R. Linder, A. J. Coates, R. D. Woodliffe, C. Alsop, A. D. Johnstone, M. Grande, A. Preece, B. Narheim, and D. T. Young, "The Cassini CAPS electron spectrometer," in *Measurement Techniques in Space Plasmas: Particles* (Geophysical Monograph, 102, American Geophysical Union, 1998), p. 257.
[27]D. McComas *et al.*, "The solar wind around pluto (SWAP) instrument aboard New Horizons," Space Sci. Rev. **140**, 261–313 (2008).

[28]J. P. McFadden, C. W. Carlson, D. Larson, M. Ludlam, R. Abiad, B. Elliott, P. Turin, M. Marckwordt, and V. Angelopoulos, "The THEMIS ESA plasma instrument and in-flight calibration," Space Sci. Rev. **141**, 277–302 (2008).
[29]J. P. McFadden *et al.*, "MAVEN Suprathermal and thermal ion compostion (STATIC) instrument," Space Sci. Rev. **195**, 199–256 (2015).
[30]D. L. Mitchell, R. P. Lin, C. Mazelle, H. Rème, P. A. Cloutier, J. E. P. Connerney, M. H. Acuña, and N. F. Ness, "Probing Mars' crustal magnetic field and ionosphere with the MGS electron reflectometer," J. Geophys. Res. **106**, 23419–23428, https://doi.org/10.1029/2000JE001435 (2001).
[31]D. L. Mitchell *et al.*, "The MAVEN solar wind electron analyzer," Space Sci. Rev. **200**, 495–528 (2016).
[32]A. O. Nier, W. B. Hanson, M. B. McElroy, A. Seiff, and N. W. Spencer, "Entry science experiments: The Viking Mars lander," Icarus **16**, 74–91 (1972).
[33]H. Nilsson *et al.*, "RPC-ICA: The ion composition analyzer of the Rosetta Plasma Consortium," Space Sci. Rev. **128**, 671–695 (2007).
[34]C. Pollock *et al.*, "Fast plasma investigation for magnetospheric multiscale," Space Sci. Rev. **199**, 331–406 (2016).
[35]J. Sauvaud *et al.*, "The IMPACT solar wind electron analyzer (SWEA)," Space Sci. Rev. **136**, 227–239 (2008).
[36]J.-A. Sauvaud *et al.*, "The Mercury electron analyzers for the Bepi Colombo mission," Adv. Space Res. **46**, 1139–1148 (2010).
[37]Y.-J. Su, J. L. Horwitz, G. R. Wilson, P. G. Richards, D. G. Brown, and C. W. Ho, "Self-consistent simulation of the photoelectron-driven polar wind from 120 km to 9 R_E altitude," J. Geophys. Res. **103**, 2279–2296, https://doi.org/10.1029/97JA03085 (1998).
[38]S. Xu *et al.*, "Martian low-altitude magnetic topology deduced from MAVEN/SWEA observations," J. Geophys. Res.: Space Phys. **122**, 1831–1852, https://doi.org/10.1002/2016JA023467 (2017).
[39]D. T. Young *et al.*, "Cassini plasma spectrometer investigation," Space Sci. Rev. **114**, 1–4 (2004).
[40]D. T. Young *et al.*, "Plasma experiment for planetary exploration (PEPE)," Space Sci. Rev. **129**, 327–357 (2007).